

CCC Publications



Adaptive Backstepping Sliding Mode Fault-Tolerant Control of Quadrotor UAV in the presence of external disturbances, uncertainties, and Simultaneous Actuator and Sensor faults

A. Ezzara*, A.Y. Ouardine, H. Ayad

Abderrahim Ezzara*

LSEEET Laboratory, Department of Applied Physics
Faculty of Science and Technology, Cadi Ayyad University, Marrakesh, Morocco
*Corresponding author: abderrahim.ezzara@ced.uca.ma

Ahmed Youssef Ouardine

Ecole Royale de l'Air, Marrakesh, Morocco
a.y.ouadine@gmail.com

Hassan Ayad

LSEEET Laboratory, Department of Applied Physics
Faculty of Science and Technology, Cadi Ayyad University, Marrakesh, Morocco
h.ayad@uca.ma

Abstract

This paper presents a new active fault-tolerant control (AFTC) strategy for quadrotor unmanned aerial vehicle (UAV) against unknown external disturbances, system uncertainties, actuator faults, and sensor faults. The study starts with a short presentation of the quadrotor's nonlinear dynamic model. Thereafter, time-varying actuator and sensor faults are simultaneously estimated by a nonlinear unknown input observer (NUIO), and to attenuate the effect of disturbances on fault estimation (FE), a \mathcal{H}_∞ performance index is used. Additionally, the proposed problem is solved using the linear matrix inequality (LMI) approach. Subsequently, a robust nonlinear adaptive backstepping sliding mode control (ABSMC) technique is proposed to manage faults amidst uncertainties and disturbances. Comparative simulations in MATLAB are provided to verify the effectiveness of the proposed strategy under different types of actuators and sensors in different scenarios.

Keywords: Active fault-tolerant control, quadrotor unmanned aerial vehicle, nonlinear dynamical model, actuator faults, sensor faults, external disturbances, uncertainties, nonlinear unknown input observer, \mathcal{H}_∞ optimization, backstepping, sliding mode control.

1 Introduction

In recent years, quadrotors as unmanned aerial vehicles (UAVs) have become increasingly vital in various fields. However, their widespread use also raises significant security concerns, including potential system failures and external disturbances. Ensuring quadrotors' reliability and resilience in the face of such challenges is critical for their effective operation in both civilian and military applications.

To address these challenges, fault-tolerant control (FTC) systems have become a focal point of research. Recent research has focused extensively on developing FTC strategies for quadrotors to address uncertainties, disturbances, actuator, and sensor faults. For instance, [1], [2], [3], and [4] addresses actuator faults and/or disturbances and uncertainties for quadrotor; however, it lacks coverage of sensor faults and uncertainties. In [5], authors study the diagnosis and compensation for sensors and actuator constant faults in a quadrotor UAV in the presence of uncertainties and external disturbances using a feedback linearization technique and a nonlinear high-gain observer. A new FTC strategy for quadrotors under time-varying sensor faults and disturbances based on a DO and a non-singular fast terminal sliding mode algorithm is proposed in [6], excluding actuator faults and uncertainties. Finally, [7] introduces a robust backstepping control strategy that includes an adaptive observer for actuator faults, missing sensor faults, disturbances, and uncertainties. Other FTC strategies are proposed in [8], [9], [10].

Existing FTC approaches for quadrotor UAVs often ignore full fault coverage, especially regarding time-varying faults. Unlike previous strategies [1]-[10], none have examined the handling of both time-varying sensor and actuator faults in the presence of uncertainties and external disturbances.

Significant study efforts have been put towards creating FTC strategies for Lipschitz nonlinear systems, with a particular focus on fault estimation (FE)-based FTC using observer-based methods [11].

This paper uses a nonlinear unknown input observer (NUIO) to estimate faults further strengthens fault-tolerant capabilities. In [12], the authors release the rank requirement by using partly decoupled disturbances, but they don't take into account the influence of system uncertainties. In [13], [14], [15], and [?], a partly decoupled UIO is suggested, however, in order to completely isolate the disturbance, it must meet a rank condition, which limits its use to many real systems. A partially decoupled UIO is proposed in [16], while only the unmatched part's FE performance is considered without considering sensor faults. Inspired by [11], a novel NUIO with disturbance attenuation without rank requirement for the quadrotor system in the presence of external disturbances, uncertainties, actuator faults, and sensor faults is proposed in this study.

This study proposes an active FE-based FTC technique for quadrotor UAV in the presence of time-varying external disturbances, uncertainties, actuator faults, and sensor faults. The strategy integrates NUIO with backstepping and SMC techniques.

The main contributions of this paper are: (1) the use of a complete nonlinear model of the quadrotor UAV taking into consideration the nonlinearities and the high order nonholonomic constraints of the system; (2) to estimate actuator and sensor faults simultaneously, a novel NUIO is developed, without any rank requirement in presence of uncertainties and external disturbances; (3) using a linear matrix inequality (LMI) formulation, the FE unit design problem is formulated as an observer-based robust control problem that can be solved by H_∞ optimization; (4) using the NUIO-based FE, an adaptive backstepping sliding mode FTC controller is constructed; (5) in addition to parametric uncertainties, wind disturbances, and noise, different time-varying additive and multiplicative actuator and sensor faults types are taking into account.

The remainder of this study is organized as follows: Section II provides a description of the quadrotor nonlinear dynamic model. Various actuator and sensor fault types are modeled in this section. In Section III, using the H_∞ optimization, a NUIO is constructed to simultaneously estimate the actuator and sensor faults amidst uncertainties and external disturbances. Section IV provides a robust ABSMC strategy to handle system failure effects in the presence of uncertainties and external disturbances. Finally, Section V shows a validation of the proposed FTC using MATLAB simulations.

2 Quadrotor Nonlinear Dynamical modeling

2.1 Quadrotor dynamical modeling

The quadrotor dynamical model can be derived using the Newton-Euler formalism. Let's introduce two reference frames, let E (O, X, Y, Z) designate an inertial frame, and B (o, x, y, z) designate a frame permanently coupled to the quadrotor body as illustrated in Figure 1. Both of them are assumed to be at the center of gravity of the quadrotor UAV.

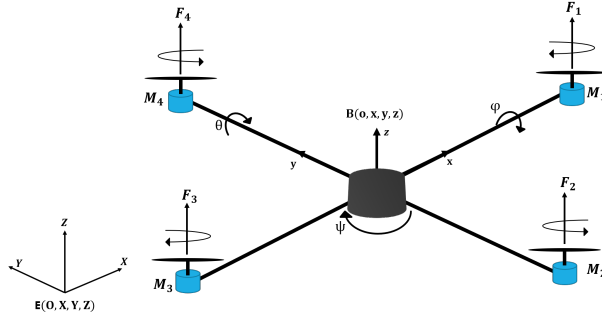


Figure 1: Quadrotor configuration

The absolute position of the quadrotor may be obtained by the three coordinates (x, y, z) and its attitude by the three Euler's angles, respectively roll ϕ , pitch θ , and yaw ψ .

The quadrotor's dynamic model, which considers the drag forces, aerodynamic friction torques, and torques due to the gyroscopic effects, is given as in [17] by:

$$\ddot{\phi} = \frac{1}{I_x} (\dot{\theta}\dot{\psi}(I_y - I_z) - K_{fax}\dot{\phi}^2 - J_r\bar{\Omega}\dot{\theta} + dU_2) \quad (1a)$$

$$\ddot{\theta} = \frac{1}{I_y} (\dot{\phi}\dot{\psi}(I_z - I_x) - K_{fay}\dot{\theta}^2 + J_r\bar{\Omega}\dot{\phi} + dU_3) \quad (1b)$$

$$\ddot{\psi} = \frac{1}{I_z} (\dot{\theta}\dot{\phi}(I_x - I_y) - K_{faz}\dot{\psi}^2 + U_4) \quad (1c)$$

$$\ddot{x} = \frac{1}{m} ((C\phi S\theta C\psi + S\phi S\psi)U_1 - K_{ftx}\dot{x}) \quad (1d)$$

$$\ddot{y} = \frac{1}{m} ((C\phi S\theta S\psi - S\phi C\psi)U_1 - K_{fty}\dot{y}) \quad (1e)$$

$$\ddot{z} = \frac{1}{m} (C\phi C\theta U_1 - K_{ftz}\dot{z}) - g \quad (1f)$$

where C is the trigonometrical function cosine, and S is the function sine, m is the total mass of the quadrotor, g is the gravity acceleration constant, I_x , I_y , and I_z are the constants inertia, K_{ftx} , K_{fty} , and K_{ftz} are the translation drag coefficients, K_{fax} , K_{fay} , and K_{faz} are the coefficients of aerodynamic friction around X , Y , and Z , d is the distance between the center of mass of the quadrotor and the rotation axis of the propellers, J_r is the rotor inertia, $\bar{\Omega}$ represents the disturbance caused by the rotor unbalance, U_1 , U_2 , U_3 , and U_4 represent the quadrotor control inputs.

Based on the angular speeds of the four rotors, the control inputs and the disturbance $\bar{\Omega}$ are expressed as follows:

$$\begin{bmatrix} U_1 \\ U_2 \\ U_3 \\ U_4 \end{bmatrix} = \begin{bmatrix} K_p & K_p & K_p & K_p \\ -K_p & 0 & K_p & 0 \\ 0 & -K_p & 0 & K_p \\ K_d & -K_d & K_d & -K_d \end{bmatrix} \begin{bmatrix} \omega_1^2 \\ \omega_2^2 \\ \omega_3^2 \\ \omega_4^2 \end{bmatrix} \quad (2)$$

$$\bar{\Omega} = \omega_1 - \omega_2 + \omega_3 - \omega_4 \quad (3)$$

where K_p is the lift coefficient, K_d is the drag coefficient, and ω_i for $i \in \{1, 2, 3, 4\}$ are the angular rotor speeds.

The control inputs remain restricted by the motors' maximum rotational speeds ω_{\max} , which are illustrative of their physical constraints:

$$\begin{aligned} 0 &\leq U_1 \leq 4K_p\omega_{\max}^2 \\ -K_p\omega_{\max}^2 &\leq U_2 \leq K_p\omega_{\max}^2 \\ -K_p\omega_{\max}^2 &\leq U_3 \leq K_p\omega_{\max}^2 \\ -2K_d\omega_{\max}^2 &\leq U_4 \leq 2K_d\omega_{\max}^2 \end{aligned} \quad (4)$$

From the equations (1d) to (1f), we can extract the expressions of the nonholonomic constraints :

$$\tan \theta = \frac{(\ddot{x} + \frac{K_{ftx}}{m}\dot{x})C_\psi + (\ddot{y} + \frac{K_{fty}}{m}\dot{y})S_\psi}{\ddot{z} + g + \frac{K_{ftz}}{m}\dot{z}} \quad (5a)$$

$$\sin \phi = \frac{(\ddot{x} + \frac{K_{ftx}}{m}\dot{x})S_\psi - (\ddot{y} + \frac{K_{fty}}{m}\dot{y})C_\psi}{\sqrt{(\ddot{x} + \frac{K_{ftx}}{m}\dot{x})^2 + (\ddot{y} + \frac{K_{fty}}{m}\dot{y})^2 + (\ddot{z} + g + \frac{K_{ftz}}{m}\dot{z})^2}} \quad (5b)$$

Nonholonomic constraints will be used to produce the desired roll (ϕ_d) and pitch (θ_d).

2.2 External disturbances modeling

In this study, we consider wind disturbances to be the primary external disturbances affecting the quadrotor's performance and stability. The Von Karman [18, 19, 20] model will be used in this paper. Wind disturbances will be noted $d_0(t)$ in the rest of this paper and given by:

$$d_0 = [d_\phi, d_\theta, d_\psi, d_x, d_y, d_z]^T \quad (6)$$

where d_ϕ , d_θ , and d_ψ represents the disturbance affecting the quadrotor's attitude. And d_x , d_y , and d_z are the disturbances along the X, Y and Z axes, respectively.

2.3 Parametric uncertainties modeling

In this study, we consider additional parameter uncertainties of the quadrotor model on the translation drag coefficients K_{ftx} , K_{fty} , and K_{ftz} , and the aerodynamic friction coefficients K_{fax} , K_{fay} , and K_{faz} . Based on the system model given by (1), the uncertainties effect can be expressed as follows:

$$\begin{aligned} \xi_\phi &= -\frac{\Delta K_{fax}}{I_x}\dot{\phi}^2, & \xi_\theta &= -\frac{\Delta K_{fay}}{I_y}\dot{\theta}^2, & \xi_\psi &= -\frac{\Delta K_{faz}}{I_z}\dot{\psi}^2, \\ \xi_x &= -\frac{\Delta K_{ftx}}{m}\dot{x}, & \xi_y &= -\frac{\Delta K_{fty}}{m}\dot{y}, & \xi_z &= -\frac{\Delta K_{ftz}}{m}\dot{z} \end{aligned} \quad (7)$$

where ΔK_{fax} , ΔK_{fay} , ΔK_{faz} , ΔK_{ftx} , ΔK_{fty} , and ΔK_{ftz} represent the uncertainties of K_{fax} , K_{fay} , K_{faz} , K_{ftx} , K_{fty} , and K_{ftz} respectively. In the rest of this paper, the uncertainty vector will be noted $\xi(x, t)$ and given by:

$$\xi = [\xi_\phi, \xi_\theta, \xi_\psi, \xi_x, \xi_y, \xi_z]^T \quad (8)$$

2.4 Actuator faults modeling

Common actuator faults include Bias fault, Loss of Effectiveness (LOE) fault, and Actuator Stuck fault [21, 22]. The combined equation for these faults can be described using:

$$f_a(t) = -\epsilon u(t) + f_{a0}(t) \quad (9)$$

where f_a is the actuator fault, u denotes the system control input, $\epsilon \in [0, 1]$ denotes the actuator gain variation coefficient, and f_{a0} is an actuator fault function. Actuator fault vector will be noted f_a in the rest of this paper and given by:

$$f_a = [f_{a1}, f_{a2}, f_{a3}, f_{a4}]^T \quad (10)$$

where f_{ai} for $i \in \{1, 2, 3, 4\}$ are the actuators faults.

2.5 Sensor faults modeling

Common sensor faults include bias fault, drift fault, loss of effectiveness (LOE), and stuck sensor fault [23, 24, 25, 26]. The combined equation for these faults can be described using:

$$f_s(t) = -\rho y(t) + f_{s0}(t) \quad (11)$$

where f_s is the sensor fault, y denotes system output, $\rho \in [0, 1]$ denotes the sensor gain variation coefficient, and f_{s0} is a sensor fault function. Actuator fault vector will be noted f_a in the rest of this paper and given by:

$$f_s = [f_{s1}, f_{s2}, f_{s3}, f_{s4}, f_{s5}, f_{s6}]^T \quad (12)$$

where f_{si} for $i \in \{1, 2, 3, 4, 5, 6\}$ are the sensor faults.

2.6 Complete nonlinear quadrotor dynamic model

Let's define the system's state vector given by:

$$x = [x_1, \dots, x_{12}]^T = [\phi, \dot{\phi}, \theta, \dot{\theta}, \psi, \dot{\psi}, x, \dot{x}, y, \dot{y}, z, \dot{z}]^T \quad (13)$$

The system output vector is given by:

$$y = \begin{bmatrix} x_1 & x_2 - f_{s1} & x_3 & x_4 - f_{s2} & x_5 & x_6 - f_{s3} \\ x_7 & x_8 - f_{s4} & x_9 & x_{10} - f_{s5} & x_{11} & x_{12} - f_{s6} \end{bmatrix}^T \quad (14)$$

From equations (1) and considering uncertainties, disturbances, actuators, and sensor faults modeled above, we obtain the following state space model:

$$\begin{aligned} \dot{x}_1 &= x_2 \\ \dot{x}_2 &= a_1 x_4 x_6 + a_2 x_2^2 + a_3 \bar{\Omega} x_4 + b_1 U_2 + f_{a1} + d_\phi + \xi_\phi \\ \dot{x}_3 &= x_4 \\ \dot{x}_4 &= a_4 x_2 x_6 + a_5 x_4^2 + a_6 \bar{\Omega} x_2 + b_2 U_3 + f_{a2} + d_\theta + \xi_\theta \\ \dot{x}_5 &= x_6 \\ \dot{x}_6 &= a_7 x_2 x_4 + a_8 x_6^2 + b_3 U_4 + f_{a3} + d_\psi + \xi_\psi \\ \dot{x}_7 &= x_8 \\ \dot{x}_8 &= a_9 x_8 + U_x \frac{U_1}{m} + d_x + \xi_x \\ \dot{x}_9 &= x_{10} \\ \dot{x}_{10} &= a_{10} x_{10} + U_y \frac{U_1}{m} + d_y + \xi_y \\ \dot{x}_{11} &= x_{12} \\ \dot{x}_{12} &= a_{11} x_{12} - g + \frac{\cos(x_1) \cos(x_3)}{m} U_1 + f_{a4} + d_z + \xi_z \end{aligned} \quad (15)$$

where

$$\begin{aligned} a_1 &= \frac{I_y - I_z}{I_x}, & a_2 &= -\frac{K_{fax}}{I_x}, & a_3 &= -\frac{J_r}{I_x}, & a_4 &= \frac{I_z - I_x}{I_y}, & a_5 &= -\frac{K_{fay}}{I_y} \\ a_6 &= \frac{J_r}{I_y}, & a_7 &= \frac{I_x - I_y}{I_z}, & a_8 &= -\frac{K_{faz}}{I_z}, & a_9 &= -\frac{K_{ftx}}{m}, & a_{10} &= -\frac{K_{fty}}{m} \\ a_{11} &= -\frac{K_{ftz}}{m}, & b_1 &= \frac{d}{I_x}, & b_2 &= \frac{d}{I_y}, & b_3 &= \frac{1}{I_z}. \end{aligned}$$

3 NUIO-based FE design

This part outlines the design of a NUIO designed to estimate actuator f_a and sensor f_s faults. The following state-space form can be employed to represent the complete model (15):

$$\begin{aligned}\dot{x}(t) &= Ax(t) + Bu(t) + \Phi(x, t) + F_a f_a(t) + Dd(t) \\ y(t) &= Cx(t) + F_s f_s(t)\end{aligned}\quad (16)$$

where $x \in \mathbb{R}^{12}$ is the system's state vector given by (13), $y \in \mathbb{R}^{12}$ is the system output vector given by (14), the control input vector is given by $u = [U_1, U_2, U_3, U_4]^T$. $f_a \in \mathbb{R}^4$ denotes the actuator fault vector given by (10), and $f_s \in \mathbb{R}^6$ denotes the sensor fault vector given by (12), $F_a \in \mathbb{R}^{12 \times 4}$ and $F_s \in \mathbb{R}^{12 \times 6}$ are known constant distribution matrices. $d \in \mathbb{R}^6$ represent lumped uncertainty that includes both external disturbances and system uncertainties. $\Phi \in \mathbb{R}^{12}$ is a continuous known nonlinear function vector. $A \in \mathbb{R}^{12 \times 12}$, $B \in \mathbb{R}^{12 \times 4}$, $C \in \mathbb{R}^{12 \times 12}$, and $D \in \mathbb{R}^{12 \times 6}$ are known constant matrices.

For the development of the considered observer, the following conditions must be satisfied [11]:

Assumption 1: The pair (A, C) is observable, the pair (A, B) is controllable, and $\text{rank}(B, F_a) = \text{rank}(B)$.

Assumption 2: The unknown input disturbances d is bounded with unknown upper bounds such that $d \in L_2[0, \infty)$.

Assumption 3: The faults f_a and f_s belong to $L_2[0, \infty)$, and f_a and f_s are continuously smooth with bounded first-time derivatives.

Assumption 4: $\Phi(x, t)$ satisfies the Lipschitz property with respect to x , such that:

$$\|\Phi(x, t) - \Phi(\hat{x}, t)\| \leq L_f \|x - \hat{x}\| \quad \forall x, \hat{x} \in \mathbb{R}^{12} \quad (17)$$

where L_f is a positive constant.

The following augmented system state space is obtained by considering actuator and sensor faults as auxiliary states.

$$\begin{aligned}\dot{\bar{x}} &= \bar{A}\bar{x} + \bar{\Phi}(A_0\bar{x}, t) + \bar{B}u + \bar{D}\bar{d} \\ y &= \bar{C}\bar{x}\end{aligned}\quad (18)$$

where

$$\begin{aligned}\bar{x} &= \begin{bmatrix} x \\ f_a \\ f_s \end{bmatrix}, \quad \bar{A} = \begin{bmatrix} A & F_a & 0 \\ 0 & 0 & 0 \\ 0 & 0 & 0 \end{bmatrix}, \quad \bar{B} = \begin{bmatrix} B \\ 0 \\ 0 \end{bmatrix}, \quad \bar{D} = \begin{bmatrix} D & 0 & 0 \\ 0 & I_4 & 0 \\ 0 & 0 & I_6 \end{bmatrix} \\ \bar{C} &= \begin{bmatrix} C & 0 & F_s \end{bmatrix}, \quad \bar{\Phi}(A_0\bar{x}, t) = \begin{bmatrix} \Phi(x, t) \\ 0 \end{bmatrix}, \quad \bar{d} = \begin{bmatrix} d \\ \dot{f}_a \\ \dot{f}_s \end{bmatrix}, \quad A_0 = \begin{bmatrix} I_{12} & 0 & 0 \end{bmatrix}\end{aligned}$$

A NUIO estimates the augmented state \bar{x} as follows:

$$\begin{aligned}\dot{z} &= Mz + Gu + N\bar{\Phi}(A_0\hat{\bar{x}}, t) + Ly \\ \hat{\bar{x}} &= z + Hy\end{aligned}\quad (19)$$

where $z \in \mathbb{R}^{22}$ is the observer system state and $\hat{\bar{x}} \in \mathbb{R}^{22}$ is the estimate of \bar{x} . The matrices $M \in \mathbb{R}^{22 \times 22}$, $G \in \mathbb{R}^{22 \times 4}$, $N \in \mathbb{R}^{22 \times 22}$, $L \in \mathbb{R}^{22 \times 12}$, and $H \in \mathbb{R}^{22 \times 12}$ are to be designed. And \hat{x} is given by $\hat{x} = \begin{bmatrix} I_{12} & 0_{12 \times 10} \end{bmatrix} \hat{\bar{x}}$, f_a and f_s could be extracted using $\begin{bmatrix} 0_{10 \times 12} & I_{10} \end{bmatrix} \hat{\bar{x}}$.

The estimation error is stated as $e = \bar{x} - \hat{\bar{x}}$. Afterward, using (18) and (19), it follows that the error time derivative is given by:

$$\begin{aligned}\dot{e} &= \dot{\bar{x}} - \dot{\hat{\bar{x}}} \\ &= (T\bar{A} - L_1\bar{C})e + (T\bar{A} - L_1\bar{C} - M)z + (T\bar{B} - G)u \\ &\quad + [(T\bar{A} - L_1\bar{C})H - L_2]y + T\bar{\Phi}(\bar{A}_0\bar{x}, t) - N\bar{\Phi}(\bar{A}_0\hat{\bar{x}}, t) + T\bar{D}\bar{d}\end{aligned}\quad (20)$$

where $T = I_{22} - H\bar{C}$ and $L = L_1 + L_2$. The observer matrices M , G , N , and L_2 are given by:

$$M = T\bar{A} - L_1\bar{C}, \quad N = T, \quad G = T\bar{B}, \quad L_2 = (T\bar{A} - L_1\bar{C})H \quad (21)$$

Matrices H and L_1 should be determined, and they are used to determine matrices M , N , G , and L .

Substituting (21) into (20), the error dynamics (20) become:

$$\dot{e} = (T\bar{A} - L_1\bar{C})e + T[\bar{\Phi}(A_0\bar{x}, t) - \bar{\Phi}(A_0\hat{\bar{x}}, t)] + T\bar{D}\bar{d} \quad (22)$$

When the effect of the system nonlinearity on the FE observer is neglected, the error (22) becomes:

$$\dot{e} = (T\bar{A} - L_1\bar{C})e + T\bar{D}\bar{d} \quad (23)$$

From equation (23), the disturbance is fully decoupled from the state/fault estimation when $\text{rank}(CD) = \text{rank}(D) + 4$ [11]. In our case, $\text{rank}(CD) = 6$ and $\text{rank}(D) = 6$, so this condition is not met. Similarly to the approach in [?], complete decoupling of the disturbance requires that $\text{rank}(\bar{C}\bar{D}) = \text{rank}(\bar{D})$. For our system, $\text{rank}(\bar{C}\bar{D}) = 12$ and $\text{rank}(\bar{D}) = 16$. This work addresses the attenuation of disturbance using resilient design, rather than complete decoupling. This discrepancy highlights the robustness of the adopted observer.

A sufficient requirement for the existence of a NUO (19), is given by Theorem 1 below:

Theorem 1. *Given a positive scalar γ , the system error (23) is asymptotically stable with H_∞ performance $\|G_{z\bar{d}}\|_\infty < \gamma$, if there exists a symmetric positive definite matrix $P \in \mathbb{R}^{22 \times 22}$, and matrices $M_1 \in \mathbb{R}^{22 \times 12}$ and $M_2 \in \mathbb{R}^{22 \times 12}$ such that*

$$\begin{bmatrix} \Omega_1 & \Omega_2 \\ \Omega_2^T & -\gamma^2 I_{16} \end{bmatrix} < 0 \quad (24)$$

where $\Omega_1 = He[P\bar{A} - M_1\bar{C}\bar{A} - M_2\bar{C}] + C_e^T C_e$ and $\Omega_2 = (P - M_1\bar{C})\bar{D}$. And $z = C_e e$ where $C_e \in \mathbb{R}^{22 \times 22}$. And $H_e(V) = V + V^\top$ for a given matrix V . Then, $H = P^{-1}M_1$ and $L_1 = P^{-1}M_2$.

Proof. Let's consider the following Lyapunov function

$$V_e = e^T Pe \quad (25)$$

where e is the error dynamics defined by (23) and P is a symmetric positive definite matrix. The time derivative of V_e along (23) is

$$\begin{aligned} \dot{V}_e &= \dot{e}^T Pe + e^T P\dot{e} \\ &= e^T He[P(T\bar{A} - L_1\bar{C})]e + He[e^T P\bar{D}\bar{d}] \end{aligned} \quad (26)$$

The H_∞ performance $\|G_{z\bar{d}}\|_\infty < \gamma$ is given by

$$J = \int_0^\infty (z^T z - \gamma^2 \bar{d}^T \bar{d}) dt < 0 \quad (27)$$

Under zero initial conditions, (27) becomes

$$\begin{aligned} J &= \int_0^\infty (z^T z - \gamma^2 \bar{d}^T \bar{d} + \dot{V}_e) dt - \int_0^\infty \dot{V}_e dt \\ &= \int_0^\infty (z^T z - \gamma^2 \bar{d}^T \bar{d} + \dot{V}_e) dt - (V_e(\infty) + V_e(0)) \\ &\leq \int_0^\infty (z^T z - \gamma^2 \bar{d}^T \bar{d} + \dot{V}_e) dt \end{aligned} \quad (28)$$

To satisfy (28), the following sufficient conditions are required:

$$J_1 = z^T z - \gamma^2 \bar{d}^T \bar{d} + \dot{V}_e < 0 \quad (29)$$

Substituting (26) into (29) yields

$$J_1 = z^T z - \gamma^2 \bar{d}^T \bar{d} + e^T \text{He}[P(T\bar{A} - L_1\bar{C})]e + \text{He}[e^T P T \bar{D} \bar{d}] \quad (30)$$

By defining $M_1 = PH$ and $M_2 = PL_1$, the condition (29) is satisfied if

$$\begin{bmatrix} \Omega_1 & \Omega_2 \\ \Omega_2^T & -\gamma^2 I_{16} \end{bmatrix} < 0 \quad (31)$$

where $\Omega_1 = \text{He}[P\bar{A} - M_1\bar{C}\bar{A} - M_2\bar{C}] + C_e^T C_e$ and $\Omega_2 = (P - M_1\bar{C})\bar{D}$. \square

4 Backstepping Sliding Mode Fault-Tolerant Controller Design

In this section, an adaptive backstepping sliding mode controller (ABSMC) based on FE provided by the NUIO shown in the previous section is presented. The proposed control approach is based on two loops, the internal loop has four control laws (U_1 , U_2 , U_3 , and U_4), and the external loop has two virtual control laws (U_x and U_y). The synoptic scheme (Figure 2) below illustrates this control strategy.

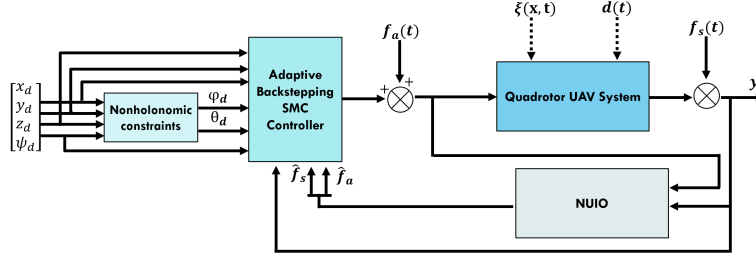


Figure 2: Synoptic scheme illustrating the control strategy.

The synthesized stabilizing control laws are as described in the following:

$$U_2 = \frac{1}{b_1} [\ddot{\phi}_d - a_1 x_4 x_6 - a_2 x_2^2 - a_3 \bar{\Omega} x_4 - k_1 \dot{e}_1 - A_1 \dot{s}_1 - s_1 - A_2 s_2 - \hat{f}_{a1} - \dot{\hat{f}}_{s1} - \hat{\Gamma}_1 \text{sign}(s_2)] \quad (32a)$$

$$U_3 = \frac{1}{b_2} [\ddot{\theta}_d - a_4 x_7 x_9 - a_5 x_8^2 - a_6 \bar{\Omega} x_7 - k_3 \dot{e}_3 - A_3 \dot{s}_3 - s_3 - A_4 s_4 - \hat{f}_{a2} - \dot{\hat{f}}_{s2} - \hat{\Gamma}_2 \text{sign}(s_4)] \quad (32b)$$

$$U_4 = \frac{1}{b_3} [\ddot{\psi}_d - a_7 x_7 x_8 - a_8 x_9^2 - k_5 \dot{e}_5 - A_5 \dot{s}_5 - s_5 - A_6 s_6 - \hat{f}_{a3} - \dot{\hat{f}}_{s3} - \hat{\Gamma}_3 \text{sign}(s_6)] \quad (32c)$$

$$U_x = \frac{m}{U_1} [\ddot{x}_d - a_9 x_{10} - k_7 \dot{e}_7 - A_7 \dot{s}_7 - s_7 - A_8 s_8 - \dot{\hat{f}}_{s4} - \hat{\Gamma}_4 \text{sign}(s_8)] \quad (32d)$$

$$U_y = \frac{m}{U_1} [\ddot{y}_d - a_{10} x_{11} - k_9 \dot{e}_9 - A_9 \dot{s}_9 - s_9 - A_{10} s_{10} - \dot{\hat{f}}_{s5} - \hat{\Gamma}_5 \text{sign}(s_{10})] \quad (32e)$$

$$U_1 = \frac{m}{c x_1 c x_2} [\ddot{z}_d - a_{11} x_{12} + g - k_{11} \dot{e}_{11} - A_{11} \dot{s}_{11} - s_{11} - A_{12} s_{12} + \hat{f}_{a4} - \dot{\hat{f}}_{s6} - \hat{\Gamma}_6 \text{sign}(s_{12})] \quad (32f)$$

We summarize all stages of calculations associated with tracking errors, sliding surfaces, and Lyapunov functions in the following manner:

Tracking errors:

$$e_i = y_i - y_{id}, \quad i \in \{1, 3, 5, 7, 9, 11\} \quad (33)$$

where y_{id} is the desired output of y_i .

Sliding surfaces equations:

$$\dot{s}_i = \dot{e}_i + k_i e_i, \quad i \in \{1, 3, 5, 7, 9, 11\} \quad (34)$$

where k_i is a positive constant for $i \in \{1, 3, 5, 7, 9, 11\}$.

Lyapunov functions:

$$V_i = \begin{cases} \frac{1}{2}s_i^2 & \text{for } i \in \{1, 3, 5, 7, 9, 11\} \\ \frac{1}{2}s_{i-1}^2 + \frac{1}{2}s_i^2 + \frac{1}{2}\beta_i \tilde{\Gamma}_i^2 & \text{for } i \in \{2, 4, 6, 8, 10, 12\} \end{cases} \quad (35)$$

where $\tilde{\Gamma}_i = \Gamma_i - \hat{\Gamma}_i$ and $\hat{\Gamma}_i$ is the estimate of Γ_i , with $\dot{\Gamma}_i = 0$. $\hat{\Gamma}_i$ is given by

$$\dot{\hat{\Gamma}}_i = \beta_i |s_i|, \quad i \in \{2, 4, 6, 8, 10, 12\} \quad (36)$$

Proof. Let's demonstrate the expression of U_2 , considering the following roll subsystem:

$$\begin{cases} \dot{x}_1 = x_2 \\ \dot{x}_2 = \Phi_1 + b_1 U_2 + f_{a1} + d_\phi + \xi_\phi \end{cases} \quad (37)$$

where $\Phi_1 = a_1 x_4 x_6 + a_2 x_2^2 + a_3 \bar{\Omega} x_4$.

The output subsystem vector is given by $[y_1 \ y_2 - f_{s1}] = [x_1 \ x_2 - f_{s1}]$, where f_{s1} is a sensor fault.

Step 1: Define the control error as $e_1 = y_1 - y_{1d} = x_1 - x_{1d}$. The sliding surface equation is:

$$s_1 = e_1 + k_1 \int e_1 dt k_1 > 0 \quad (38)$$

The Lyapunov function chosen is:

$$V_1 = \frac{1}{2}s_1^2 \quad (39)$$

The time derivative of V_1 is:

$$\begin{aligned} \dot{V}_1 &= s_1 \dot{s}_1 = s_1(\dot{e}_1 + k_1 e_1) \\ &= s_1(y_2 + f_{s1} - \dot{x}_{1d} + k_1 e_1) \end{aligned} \quad (40)$$

The virtual control input is chosen as:

$$(y_2)_d = \alpha_1 = \dot{x}_{1d} - k_1 e_1 - A_1 s_1 - \hat{f}_{s1} - \alpha_{s1} \quad (41)$$

α_{s1} is a nonlinear damping remains to be determined. Substituting the virtual control value of $(y_2)_d$, \dot{V}_1 becomes:

$$\dot{V}_1 = -A_1 s_1^2 - s_1(\alpha_{s1} - \tilde{f}_{s1}) \quad (42)$$

where $\tilde{f}_{s1} = f_{s1} - \hat{f}_{s1}$. Choosing $\alpha_{s1} = k_{s1} \text{sign}(s_1)$, where $\text{sign}(\cdot)$ denotes the sign function and $k_{s1} > 0$, Equation (42) becomes:

$$\begin{aligned} \dot{V}_1 &= -A_1 s_1^2 - s_1(k_{s1} \text{sign}(s_1) - \tilde{f}_{s1}) \\ &\leq -A_1 s_1^2 - |s_1|(k_{s1} - |\tilde{f}_{s1}|) \end{aligned} \quad (43)$$

Suppose there exists a positive constant k_{s1} , such that:

$$|\tilde{f}_{s1}| \leq k_{s1} \quad (44)$$

Finally, the equation (43) becomes

$$\dot{V}_1 \leq -A_1 s_1^2 \leq 0 \quad (45)$$

Step 2: As α_1 is not a real command, we define the following tracking-error variable between the state variable y_2 and its desired value α_1 . The second sliding surface is:

$$s_2 = y_2 - \alpha_1 = y_2 - \dot{x}_{1d} + k_1 e_1 + A_1 s_1 + \hat{f}_{s1} + \alpha_{s1} \quad (46)$$

The derivative of s_2 over time is:

$$\begin{aligned} \dot{s}_2 &= \dot{y}_2 - \ddot{x}_{1d} + k_1 \dot{e}_1 + A_1 \dot{s}_1 + \dot{\hat{f}}_{s1} + \dot{\alpha}_{s1} \\ &= \dot{x}_2 - \dot{f}_{s1} - \ddot{x}_{1d} + k_1 \dot{e}_1 + A_1 \dot{s}_1 + \dot{\hat{f}}_{s1} + \dot{\alpha}_{s1} \\ &= \Phi_1 + b_1 U_2 + f_{a1} + d_\phi + \xi_\phi - \dot{f}_{s1} - \ddot{x}_{1d} + k_1 \dot{e}_1 + A_1 \dot{s}_1 + \dot{\hat{f}}_{s1} + \dot{\alpha}_{s1} \end{aligned} \quad (47)$$

Based on the principle of certain equivalence, f_{a1} and d_ϕ are replaced by their estimates. Using the sliding surface in equation (47), the input control U_2 is given by:

$$U_2 = \frac{1}{b_1} \left[\ddot{\phi}_d - \Phi_1 - k_1 \dot{e}_1 - A_1 \dot{s}_1 - s_1 - A_2 s_2 - \hat{f}_{a1} - \dot{\hat{f}}_{s1} - \hat{\Gamma}_1 \text{sign}(s_2) \right] \quad (48)$$

where $\dot{\hat{\Gamma}}_1 = \beta_1 |s_2|$, and β_1 is a positive constant. Replacing U_2 in equation (47), \dot{s}_2 becomes

$$\dot{s}_2 = \tilde{f}_{a1} + d_\phi + \xi_\phi - \dot{f}_{s1} - \dot{\alpha}_{s1} - s_1 - \hat{\Gamma}_1 \text{sign}(s_2) - A_2 s_2 \quad (49)$$

The presence of the terms \tilde{f}_{a1} , d_ϕ , ξ_ϕ , \dot{f}_{s1} , and $\dot{\alpha}_{s1}$ in the expression of \dot{s}_2 does not assert the system stability. To overcome this obstacle, we increase the function of Lyapunov by adding a square term involving $\tilde{\Gamma}_1$.

$$V_2 = \frac{1}{2} (s_1^2 + s_2^2) + \frac{1}{2\beta_1} \tilde{\Gamma}_1^2 \quad (50)$$

where $\tilde{\Gamma}_1 = \Gamma_1 - \hat{\Gamma}_1$, and $\hat{\Gamma}_1$ is the estimate of Γ_1 (assuming $\dot{\Gamma}_1 \approx 0$). Its derivative is

$$\begin{aligned} \dot{V}_2 &= s_1 \dot{s}_1 + s_2 \dot{s}_2 + \frac{1}{\beta_1} \tilde{\Gamma}_1 \dot{\tilde{\Gamma}}_1 \\ &= s_1 (s_2 - A_1 s_1) + s_2 \dot{s}_2 - (\Gamma_1 - \hat{\Gamma}_1) |s_2| \\ &= -A_1 s_1^2 - A_2 s_2^2 + s_2 (\tilde{f}_{a1} + d_1 + \xi_1 - \dot{f}_{s1} - \dot{\alpha}_{s1} - \hat{\Gamma}_1 \text{sign}(s_2)) - \Gamma_1 |s_2| \\ &\leq -A_1 s_1^2 - A_2 s_2^2 + \hat{\Gamma}_1 (|s_2| - s_2 \text{sign}(s_2)) + |s_2| (\tilde{f}_{a1} + d_1 + \xi_1 - \dot{f}_{s1} - \dot{\alpha}_{s1} - \Gamma_1) \\ &\leq -A_1 s_1^2 - A_2 s_2^2 + |s_2| (|\tilde{f}_{a1} + d_\phi + \xi_\phi - \dot{f}_{s1} - \dot{\alpha}_{s1}| - \Gamma_1) \end{aligned} \quad (51)$$

Assumption 5: There exists an unknown parameter $\Gamma_1 > 0$, such that:

$$|\tilde{f}_{a1} + d_\phi + \xi_\phi + \dot{f}_{s1} - \dot{\alpha}_{s1}| \leq \Gamma_1 \quad (52)$$

Thus, $\dot{V}_2 \leq 0$ if $|\tilde{f}_{a1} + d_\phi + \xi_\phi + \dot{f}_{s1} - \dot{\alpha}_{s1}| \leq \Gamma_1$.

To avoid non-differentiability and chattering phenomena, the sign function will be replaced by a smooth function. A suitable choice is:

$$\text{sign}(s, \delta) = \frac{s}{\|s\| + \delta} \quad (53)$$

where δ is a small positive constant. \square

5 Simulation Results and Analysis

To evaluate the performance of the proposed FTC, we executed simulations in the MATLAB-SIMULINK® environment across three scenarios. Scenario 1 involved trajectory tracking with only wind disturbances and uncertainties. Scenario 2 introduced actuator faults, wind disturbances, and uncertainties, while Scenario 3 included both actuator, sensor faults, wind disturbances, and uncertainties. The integration time step is chosen as 0.001s. The quadrotor subject of our study is the Draganfly IV manufactured by “Draganfly Innovations”. Parameter identification is studied in [27] and summarized below:

m	$= 400 \text{ g}$
g	$= 9.81 \text{ m/s}^2$
d	$= 20.5 \text{ cm}$
K_P	$= 2.9842 \times 10^{-5} \text{ N/rad/s}$
K_d	$= 3.232 \times 10^{-7} \text{ N.m/rad/s}$
(I_x, I_y, I_z)	$= (3.8278, 3.8278, 7.1345) \times 10^{-3} \text{ N.m/rad/s}^2$
$(K_{ftx}, K_{fty}, K_{ftz})$	$= (3.2, 3.2, 4.8) \times 10^{-2} \text{ N/m/s}$
$(K_{fax}, K_{fay}, K_{faz})$	$= (5.567, 5.567, 6.354) \times 10^{-4} \text{ N/rad/s}$
J_r	$= 2.8385 \times 10^{-5} \text{ N.m/rad/s}^2$

For the Observer design purpose, choosing $Y_1 = 0.3 \cdot \mathbf{1}_{4 \times 12}$, $C_1 = I_{22}$, $\gamma = 0.5$, and $L_f = 35$.

To achieve realistic simulations, additive noise modeled as Gaussian random variables $\mathcal{N}(\mu, \sigma^2)$ with means μ and variances σ are introduced during all simulations of scenarios 2 and 3 in both actuator and sensor faults.

5.1 Trajectory tracking with only external disturbance and uncertainties

In Simulink, the "Von Karman Wind Turbulence Model" block was used to produce time-varying wind gusts as output. In our models, the mean wind speeds are of 5 m/s for attitude and 8 m/s for position.

Assuming that K_{ftx} , K_{fty} , and K_{ftz} , as well as K_{fax} , K_{fay} , and K_{faz} are subject to a parametric uncertainty of 25% (for example, $\Delta K_{ftx} = 0.25K_{ftx}$).

The figure 3 illustrates the varying velocity of wind disturbances over time, showcasing the intensity and fluctuations that the quadrotor must contend with during flight.

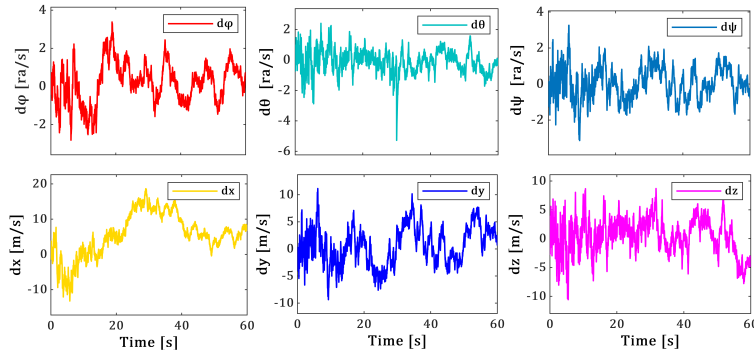


Figure 3: Wind disturbances velocity profile using Von Kármán model.

Figure 4 display excellent tracking accuracy and stability despite wind disturbances and uncertainties, showing the efficiency of the suggested approach under complicated environmental and parametric conditions.

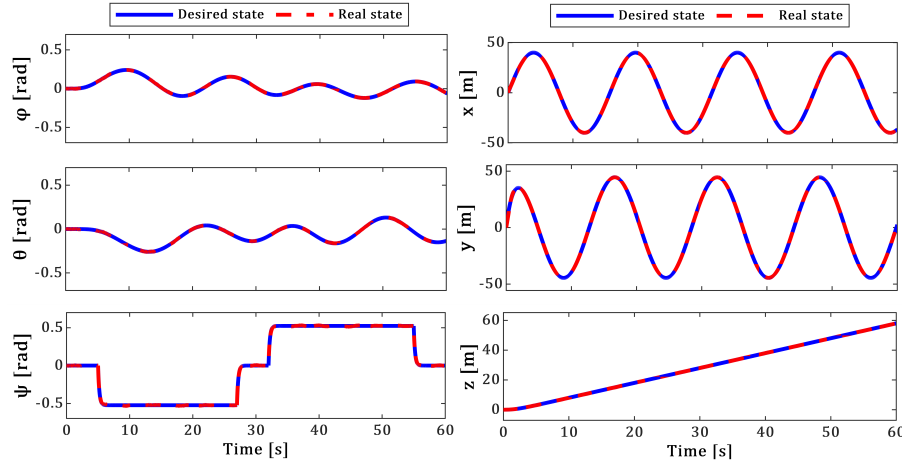


Figure 4: Attitude and position tracking in the presence of uncertainties and wind disturbances.

5.2 Trajectory tracking in presence of actuator faults

In this case (scenario 2), in addition to wind disturbances and uncertainties, the quadrotor is suffering from multiple actuator faults in two actuators. The fault profile is resumed in table 1. Where $W(t) = \sum_{k=0}^5 0.4^k \cos(3^k \pi t)$ is the Weierstrass function. While the faults under consideration are often considered differentiable, we propose a Weierstrass function-type fault that is smooth but non-differentiable.

Additive noise is added to the actuator faults. $\mathcal{N}_{a1}(0.05, 0.05^2)$ is added to f_{a1} , and $\mathcal{N}_{a4}(0.005, 0.005^2)$ is added to f_{a4} , with a sampling period of 0.05s for both.

The corresponding FE of f_{a1} and f_{a4} in each actuator is shown in Figure 5. It demonstrates good FE accuracy with RMSE for f_{a1} (ϕ) and f_{a4} (z) hovering around 10^{-14} .

Table 1: Actuator faults f_{a1} and f_{a4} profile

$f_{a1}(\phi)$	$f_{a4}(z)$	Occurrence time	Fault type
0	0	$0 \leq t < 10$ s	Fault free
5	5	$10 \leq t < 20$ s	Bias fault
$-0.4U_2(t)$	$-0.3U_1(t)$	$20 \leq t < 30$ s	LOE
$-U_2(t) + 5$	$-U_1(t) + 5$	$30 \leq t < 40$ s	Actuator Stuck
$-U_2(t) - 5$	$-U_1(t) - 5$	$40 \leq t < 50$ s	Actuator Stuck
$2W(t)$	$1W(t)$	$50 \leq t < 60$ s	Weierstrass function

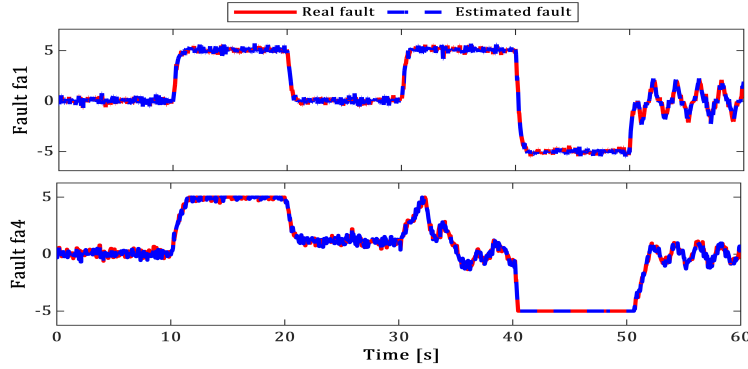


Figure 5: Actuator fault estimation.

The trajectory tracking for attitude and position of the quadrotor under scenario 2 is illustrated in Figure 6. It can be seen from Figure 6 that the desired and the real state are matched perfectly even after the occurrence of actuator faults, which clearly illustrates the good performance and robustness of the control strategy against actuator faults.

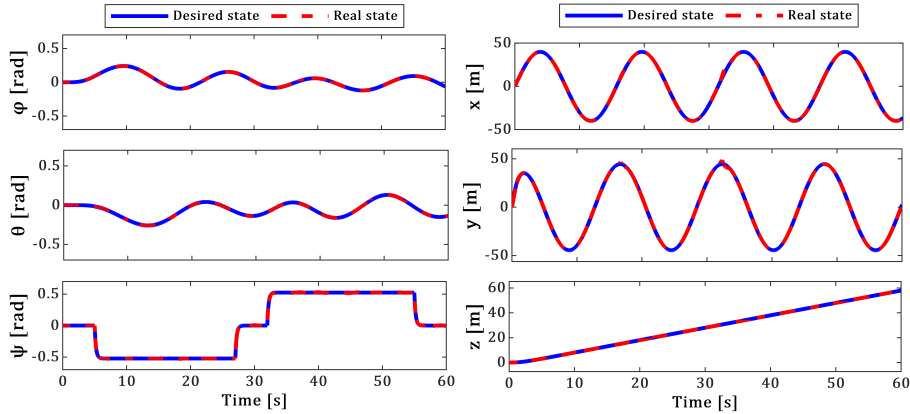


Figure 6: Trajectory tracking in the presence of actuator faults, uncertainties, and wind disturbances.

5.3 Trajectory tracking in presence of actuator and sensor faults

In this case (scenario 3), in addition to wind disturbances, parametric uncertainties, and actuator faults, the quadrotor is suffering from multiple sensor faults ($f_{s1}(\phi)$, $f_{s4}(x)$, $f_{s5}(y)$). The actuator faults profile remains the same as injected in the previous section, while the sensor fault profile with different sensor fault types occurring sequentially is described in table 2. Additive gaussian noise $\mathcal{N}_{s4}=\mathcal{N}_{s5}=(0.01, 0.01^2)$ is added to f_{s4} and f_{s5} , with a sampling period of 0.02s.

To test the robustness of the proposed technique, we examined the impact of a simultaneous actuator and sensor fault on the roll, as well as the influence of a Weierstrass function fault on all the considered sensor faults.

Table 2: Sensor faults $f_{s1}(\phi)$, $f_{s4}(x)$, $f_{s5}(y)$ profile

$f_{s1}(\phi)$	$f_{s4}(x)$	$f_{s5}(y)$	Occurrence time	Fault type
0	0	0	$0 \leq t < 10$ s	Fault free
1	5	5	$10 \leq t < 20$ s	Bias fault
$0.1t$	$0.6t$	$0.6t$	$20 \leq t < 30$ s	Drift fault
$-0.6\dot{\phi}(t)$	$-0.25\dot{x}(t)$	$-0.25\dot{y}(t)$	$30 \leq t < 40$ s	LOE fault
$-\dot{\phi}(t) + 1$	$-\dot{x}(t) + 5$	$-\dot{y}(t) + 5$	$40 \leq t < 50$ s	Stuck Sensor fault
$0.4W(t)$	$4W(t)$	$4W(t)$	$50 \leq t < 60$ s	Weierstrass function fault

Sensor fault estimation of f_{s1} , f_{s4} , and f_{s5} is shown in Figure 7. It illustrates the precise estimation of sensor faults. The results highlight the robustness of the capability of the developed NUIO to accurately estimate these faults without being significantly impacted by these disturbances, with RMSE for f_{s1} , f_{s4} , and f_{s5} remaining close to zero.

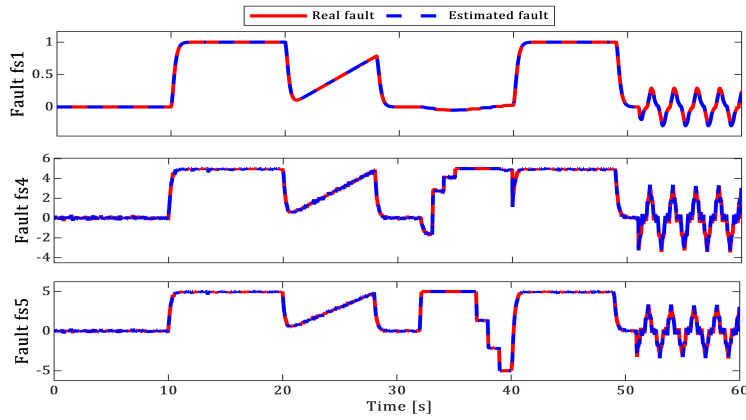
Figure 7: Sensor FE of f_{s1} , f_{s4} , and f_{s5}

Figure 8 illustrates the system's tracking performance under scenario 3.

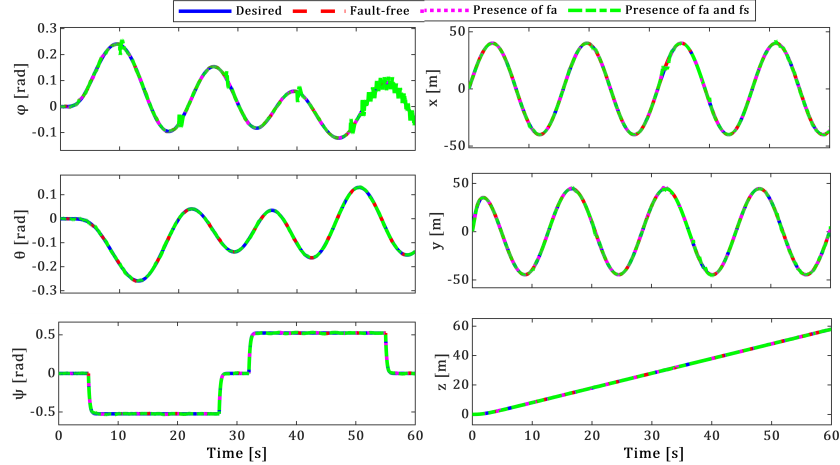


Figure 8: Trajectories along attitude and position in the presence of actuator and sensor faults

Despite the presence of some fluctuations in the states, particularly in ϕ , x , and y , the tracking remains robust, showcasing the effectiveness of the proposed FTC strategy.

The figure 9 illustrates the global trajectory of the quadrotor in 3D along the (X , Y , Z) axis in the presence of actuator and sensor faults. Despite some fluctuations, it reveals a stable and accurate flight path, even with the challenges posed by faults.

The tracking errors of the attitude, and the position are given by Figure 10. The plots reveal that

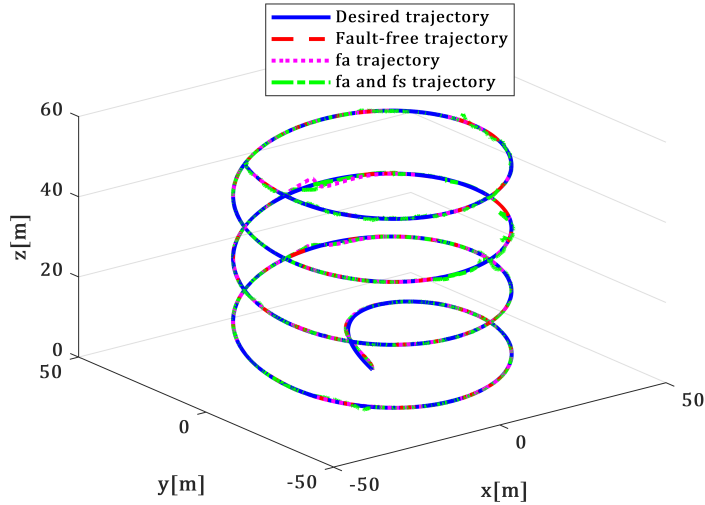


Figure 9: Global trajectory of the quadrotor in 3D in presence of actuators and sensor faults.

the tracking errors for θ , ψ , and z are small across all scenarios, while errors for ϕ , x , and y increase significantly in the presence of both actuator and sensor faults. Despite that, the attitude mean error remains below 10^{-5} rad and the position mean error stays under 10^{-3} m.

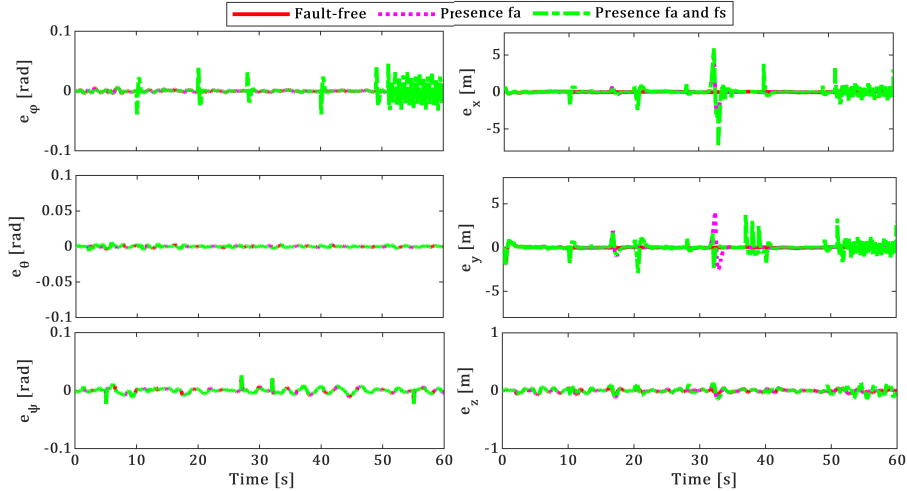


Figure 10: Tracking errors in the quadrotor's attitude and position when there are actuator and sensor faults.

Figure 11 illustrates the control inputs U_1 , U_2 , U_3 , and U_4 of our system in the presence of actuator and sensor faults (Scenario 3). The control signals generated by this strategy are both physically realizable and robust, reflecting the practicality of the proposed FTC approach. Additionally, the low energy consumption is maintained through small control inputs, highlighting the efficiency of the control method.

The Table 3 comparing the RMSE for the three different scenarios provides valuable insights into the quadrotor's performance.

In Scenario 1, where only external disturbances and uncertainties are present, the system shows minimal deviation in both attitude and position of the RMSE. In Scenario 2, where actuator faults are introduced, the attitude RMSE values remain nearly identical to those in Scenario 1, showing that the attitude control is robust against actuator faults. In Scenario 3, both actuator and sensor faults are present. The attitude RMSE values remain nearly identical to those in Scenario 2. The x and y coordinates RMSE values increase, while the z coordinate RMSE remain nearly identical to those in Scenario 2.

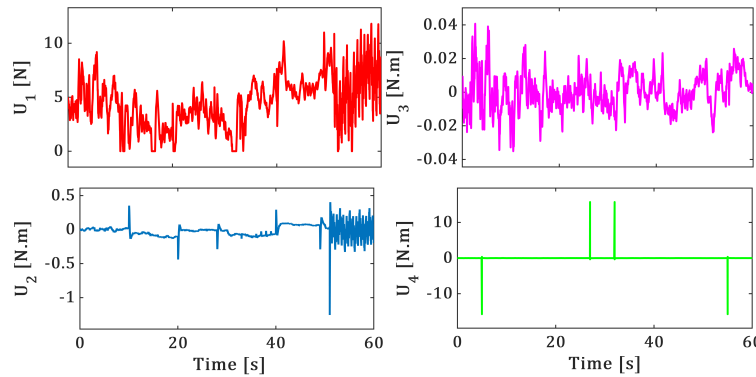


Figure 11: Control inputs of actuators in presence of actuator and sensor faults

Table 3: Root Mean Square Error (RMSE) values for attitude (on rad) and position (on m) in different scenarios

Scenario	RMSE (ϕ)	RMSE (θ)	RMSE (ψ)	RMSE (x)	RMSE (y)	RMSE (z)
Scenario 1	1.38×10^{-3}	1.45×10^{-3}	4.66×10^{-3}	1.22×10^{-3}	1.24×10^{-3}	2.44×10^{-2}
Scenario 2	1.38×10^{-3}	1.45×10^{-3}	4.66×10^{-3}	2.80×10^{-2}	2.75×10^{-2}	2.66×10^{-2}
Scenario 3	3.38×10^{-3}	1.45×10^{-3}	4.66×10^{-3}	0.15	0.16	2.80×10^{-2}

6 Conclusion

The present study introduces a new FE-based active FTC based on a new NUIO and a backstepping SMC technique for quadrotor UAV to handle wind disturbances, parametric uncertainties, noise, actuator faults, and sensor faults. The study begins with a short description of the quadrotor's nonlinear dynamic model, which takes into consideration the nonlinearities and high-order nonholonomic constraints of the system. In the presence of uncertainties and external disturbances, a novel NUIO is proposed to estimate actuator and sensor faults simultaneously, without requiring a rank condition; the FE unit design problem is formulated as an observer-based robust control problem, and it is solved using H_∞ optimization in an LMI formulation. An adaptive backstepping sliding mode FTC controller using the NUIO-based FE is constructed, and in addition to parametric uncertainties and wind disturbances, different time-varying additive and multiplicative actuator and sensor fault types are taken into account under a noisy environment.

To evaluate the performance of the proposed controller, we executed simulations in MATLAB across three scenarios. Based on the analysis of three scenarios with different faults and disturbances, the proposed FTC system shows varying performance.

The results of the simulation clearly illustrate the good performance of the adopted strategy, as it made it possible to precisely estimate the faults and to ensure stability and trajectory tracking.

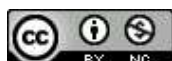
In conclusion, the proposed FTC techniques demonstrate robust performance in mitigating the effects of wind disturbances and uncertainties, maintaining acceptable tracking accuracy in various scenarios, and addressing different environmental challenges effectively.

References

- [1] Baldini, A., Felicetti, R., Freddi, A., Monteriù, A., "Fault-Tolerant Control of a Variable-Pitch Quadrotor under Actuator Loss of Effectiveness and Wind Perturbations," *Sensors and Transducers*, vol. 23, no. 10, p. 4907, May 2013.
- [2] Nguyen, N., Hong, S., "Fault-Tolerant Control of Quadcopter UAVs Using Robust Adaptive Sliding Mode Approach," *Energies*, vol. 12, p. 95, December 2018.

- [3] Nguyen, N., Hong, S., "Active Fault-Tolerant Control of a Quadcopter against Time-Varying Actuator Faults and Saturation Using Sliding Mode Backstepping Approach," *Applied Sciences*, vol. 9, p. 4010, September 2019.
- [4] Wang, B., Yu, X., Mu, L., Zhang, Y., "Disturbance observer-based adaptive fault-tolerant control for a quadrotor helicopter subject to parametric uncertainties and external disturbances," *Mechanical Systems and Signal Processing*, vol. 120, pp. 727-743, April 2019.
- [5] Ma, H., Liu, Y., Li, T., Yang, G.-H., "Nonlinear High-Gain Observer-Based Diagnosis and Compensation for Actuator and Sensor Faults in a Quadrotor Unmanned Aerial Vehicle," *IEEE Transactions on Industrial Informatics*, vol. 15, no. 1, pp. 550-562, August 2019.
- [6] Nguyen, N.-P., Pitakwatchara, P., "Attitude Fault-Tolerant Control of Aerial Robots with Sensor Faults and Disturbances," *Drones*, vol. 7, p. 156, February 2023.
- [7] Ezzara, A., Ouadine, A. Y., Ayad, H., "Adaptive Observer-based Fault-Tolerant Control for Actuator Faults in Quadrotor UAV," in *2024 International Conference on Global Aeronautical Engineering and Satellite Technology (GAST)*, pp. 1-5, 2024.
- [8] Ouadine, A. Y., Mjahed, M., Ayad, H., El Kari, A., "UAV Quadrotor Fault Detection and Isolation Using Artificial Neural Network and Hammerstein-Wiener Model," *Studies in Informatics and Control*, vol. 29, no. 3, pp. 317-328, 2020.
- [9] Zou, P., Hou, B., Jiang, L., Zhang, Z., "Bearing Fault Diagnosis Method Based on EEMD and LSTM," *International Journal of Computers Communications and Control*, vol. 15, no. 1, 2020.
- [10] Moldovan, O., Ghincu, R., Moldovan, A., Noje, D., Tarca, R., "Fault Detection in Three-phase Induction Motor based on Data Acquisition and ANN based Data Processing," *International Journal of Computers Communications and Control*, vol. 17, no. 3, 2022.
- [11] Lan, J., Patton, R. J., "Integrated fault estimation and fault-tolerant control for uncertain Lipschitz non-linear systems," *International Journal of Robust and Nonlinear Control*, vol. 27, no. 5, pp. 761-780, 2016.
- [12] Gao, Z., Liu, X., Chen, M., "Unknown Input Observer Based Robust Fault Estimation for Systems Corrupted by Partially-Decoupled Disturbances," *IEEE Transactions on Industrial Electronics*, vol. 63, pp. 1-1, January 2015.
- [13] Chen, J., Patton, R., Zhang, H.-Y., "Design of unknown input observers and robust fault detection filters," *International Journal of Control*, vol. 63, pp. 85-105, February 2007.
- [14] Chen, W., Saif, M., "Unknown input observer design for a class of nonlinear systems: An LMI approach," in *Proceedings of the American Control Conference*, vol. 2006, pp. 5 pp.-, July 2006.
- [15] Xia, J., Jiang, B., Zhang, K., "UIO-Based Practical Fixed-Time Fault Estimation Observer Design of Nonlinear Systems," *Symmetry*, vol. 14, p. 1618, August 2022.
- [16] Hashemi, M., Egoli, A., Naraghi, M., Tan, C., "Saturated Fault Tolerant Control Based on Partially Decoupled Unknown-Input Observer: A New Integrated Design Strategy," *IET Control Theory and Applications*, July 2019.
- [17] Bouadi, H., Tadjine, M., Bouchoucha, M., "Modelling and stabilizing control laws design based on backstepping for an UAV type-quadrotor," *IFAC Proceedings Volumes*, vol. 40, no. 15, pp. 245-250, 2007.
- [18] Li, F., Song, W.-P., Song, B., Jiao, J., "Dynamic Simulation and Conceptual Layout Study on a Quad-Plane in VTOL Mode in Wind Disturbance Environment," *International Journal of Aerospace Engineering*, vol. 2022, pp. 1-24, January 2022.

- [19] Li, F., Song, W.-P., Song, B., Zhang, H., "Dynamic modeling, simulation, and parameter study of electric quadrotor system of Quad-Plane UAV in wind disturbance environment," *International Journal of Micro Air Vehicles*, vol. 13, January 2021.
- [20] Cole, K., "Reactive trajectory generation and formation control for groups of UAVs in windy environments," Washington, 2018.
- [21] Boskovic, J., Mehra, R., "Stable adaptive multiple model-based control design for accommodation of sensor failures," in *Proceedings of the American Control Conference*, vol. 3, pp. 2046 - 2051, February 2002.
- [22] Jinghui, P., Lili, Q., Kaixiang, P., "Sensor and Actuator Fault Diagnosis for Robot Joint Based on Deep CNN," *Entropy*, vol. 23, p. 751, June 2021.
- [23] Dai, X., Qin, F., Gao, Z., Pan, K., Busawon, K., "Model-based on-line sensor fault detection in Wireless Sensor Actuator Networks," in *2015 IEEE 13th International Conference on Industrial Informatics (INDIN)*, pp. 556-561, 2015.
- [24] Ahmed, A. A., Khalid, H., "A Review of Fault Tolerant Control Systems: Advancements and Applications," *Measurement*, vol. 143, pp. 58-68, April 2019.
- [25] Balaban, E., Saxena, A., Bansal, P., Goebel, K. F., Curran, S., "Modeling, Detection, and Disambiguation of Sensor Faults for Aerospace Applications," *IEEE Sensors Journal*, vol. 9, no. 12, pp. 1907-1917, 2009.
- [26] Silva, J., Saxena, A., Balaban, E., Goebel, K., "A knowledge-based system approach for sensor fault modeling, detection and mitigation," *Expert Systems with Applications*, vol. 39, pp. 10977-10989, September 2012.
- [27] Derafa, L., Madani, T., Benallegue, A., "Dynamic modelling and experimental identification of four rotor helicopter parameters," in *2006 IEEE International Conference on Industrial Technology*, pp. 1834-1839, 2006.



Copyright ©2024 by the authors. Licensee Agora University, Oradea, Romania.

This is an open access article distributed under the terms and conditions of the Creative Commons Attribution-NonCommercial 4.0 International License.

Journal's webpage: <http://univagora.ro/jour/index.php/ijccc/>



This journal is a member of, and subscribes to the principles of,
the Committee on Publication Ethics (COPE).

<https://publicationethics.org/members/international-journal-computers-communications-and-control>

Cite this paper as:

Ezzara, A.; Ouadine, A.Y.;Ayad, H. (2024). Adaptive-Backstepping-Sliding-Mode Fault-Tolerant Control of Quadrotor UAV in presence of external disturbances, uncertainties, and Simultaneous Actuator and Sensor faults,*International Journal of Computers Communications & Control*, 19(1), 4xyz, 2024.

<https://doi.org/10.15837/ijccc.2024.1.4xyz>